

YbCo₂: Large Magnetic Entropy Change per Volume in Yb-based Metallic Magnetic Refrigerants for Sub-Kelvin Temperature

Yasuyuki Shimura,^{1, a)} Ryoma Yokoo,¹ Kanta Watanabe,¹ Hiroto Furuie,¹ Naohito Tsujii,² Kazunori Umeo,³ and Takahiro Onimaru¹

¹⁾Department of Quantum Matter, Graduate School of Advanced Science and Engineering, Hiroshima University, Higashi-Hiroshima 739-8530, Japan

²⁾Research Center for Materials Nanoarchitectonics (MANA), National Institute for Materials Science (NIMS), 1-2-1 Sengen, Tsukuba, Ibaraki 305-0047, Japan

³⁾Department of Low Temperature Experiment, Integrated Experimental Support/Research Division, N-BARD, Hiroshima University, Higashi-Hiroshima 739-8526, Japan

(Dated: 4 August 2025)

A Yb-based intermetallic compound YbCo₂ exhibiting a magnetic-field-induced order is known to show a giant specific heat divided by temperature, $C/T \sim 6.5 \text{ J/K}^2\text{mol}$, around 0.3 K. We investigate the potential of this substance as the magnetic refrigerants by measuring the thermodynamic properties down to 0.1 K. The entropy change per volume by applying magnetic field of 3 T is found to be $-\Delta S_M \sim 0.15 \text{ J/K cm}^3$ around 1 K. This value is particularly large in the Yb-based metallic magnetic refrigerants to provide the sub-Kelvin temperature. In addition, we demonstrate that a 2.2 gram sample is cooled down to 0.26 K by the adiabatic demagnetization refrigeration from 1.8 K and 12 T. This cooling performance is attributed to the ground state, at zero field, locating around the boundary between the field-induced ordered phase and the paramagnetic one. Our study clarifies the utility of the sub-Kelvin magnetic refrigerants which combine the large $-\Delta S_M$ and the high thermal conductivity of metal.

Adiabatic demagnetization refrigeration (ADR) is a technique to cool down by demagnetizing the magnetic refrigerants on the quasi-adiabatic environments. Since this technique needs only a magnet and magnetic materials as the refrigerants, we can reach the cryogenic temperature below 1 K without complex refrigerators using precious ³He. Though paramagnetic salts including 3d-transition metals have been used as the cryogenic magnetic refrigerants for decades, it is not convenient to use them because of the chemical instability^{1,2}. In recent years, various stable magnetic refrigerants including rare-earth ions have been studied. The low magnetic-transition temperature T_M in rare-earth ions retains the magnetic entropy used for magnetic refrigeration around absolute zero.

The performance as the magnetic refrigerants is evaluated by two parameters of the *adiabatic temperature change*, ΔT_{ad} , and the *magnetic entropy change*, $-\Delta S_M$. The former is defined as $\Delta T_{\text{ad}} = T_i - T_f$, where T_i (T_f) indicates the initial (final) temperature before (after) demagnetization in the ADR experiments. The value of $-\Delta S_M$ is evaluated as the difference between the entropy under the zero field and the magnetic field. We often need to mount the magnetic refrigerants on the narrow space in a refrigerator. In addition, the spatial area where the magnetic field is applied is limited. Therefore, the magnitude of $-\Delta S_M$ per volume is of importance for the real application.

Main route to increase the amount of $-\Delta S_M$ is focusing on the Gd-based compounds since a Gd³⁺ has an entropy of $\ln 8 = 3 \ln 2$ arising from the spin $S = 7/2$. This value is 3 times as large as that in the ground state doublet realized in most other rare-earth ions affected by the crystalline electric field. Indeed, some magnetic refrigerants of Gd-based

oxides/fluoride where T_M is suppressed by the geometrical frustration effect exhibit large $-\Delta S_M$ exceeding 0.1-0.2 J/K cm³³⁻⁹. Instead of such a large $-\Delta S_M$, if we demand T_f below ~ 0.1 K, the Yb-based oxides should be selected⁹⁻¹².

Another significant point to cool down to below 1 K is the thermal conductivity of the magnetic refrigerants because the thermal conductivity in the insulators mentioned above sharply decays as a power of temperature on cooling. In this point, Yb-based intermetallic compounds are advantageous as the cryogenic magnetic refrigerants to cool down to ~ 0.2 K¹³⁻¹⁶. The strongly localized nature of 4f electrons in the heavy rare-earth ion Yb³⁺ (4f¹³) results in the low T_M related to T_f . Another advantage peculiar to the strongly correlated metals including Yb or Ce is that T_f can be further lowered with the chemical substitution by tuning the ground state to the quantum critical points where T_M is absolute zero¹⁷⁻¹⁹.

Thus, Yb-based intermetallic compounds are advantageous as the cryogenic magnetic refrigerants because of the low T_f and the high thermal conductivity. In this paper, we report the performance of YbCo₂ as magnetic refrigerants. YbCo₂ is one of the C15 Laves-phase compounds with the cubic MgCu₂-type structure²⁰. The specific heat divided by temperature, C/T , divergently increases on cooling and exhibits a maximum at ~ 0.3 K, where the value of C/T is $\sim 6.5 \text{ J/K}^2\text{mol}$ ^{21,22}. A magnetically ordered state appears to set in at 0.3 K as inferred from the zero-field μSR experiments. This giant C/T and the density of Yb, accounting for 1/3 in the constituent atoms, are expected to provide the sizable entropy per volume at zero field. Notably, YbCo₂ exhibits a field-induced order above 1 T and 2 K²¹. In this field-induced phase, both moments in Yb and Co order magnetically²². Since the field-induced order takes away the entropy under magnetic field around absolute zero, enhancement of $-\Delta S_M$ is expected.

Polycrystalline samples of YbCo₂ were prepared from Yb ingots and Co powder. An open tungsten crucible containing

^{a)}Electronic mail: simu@hiroshima-u.ac.jp

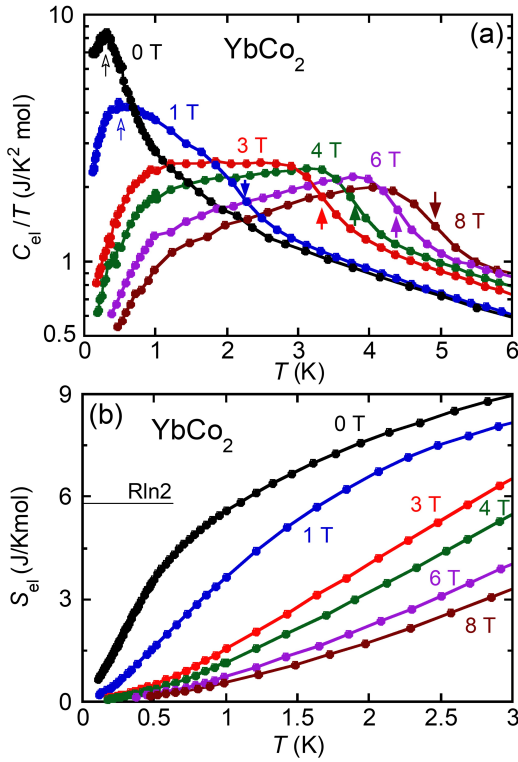


FIG. 1. (a) Electronic specific heat divided by temperature C_{el}/T under the magnetic field up to 8 T in YbCo₂. The closed and open arrows show the drops in C_{el}/T on heating by the field-induced phase transition and the peak, respectively. (b) Electronic entropy S_{el} derived from C_{el}/T .

them was encapsulated in a quartz ampoule under Ar atmosphere. This crucible in this quartz ampoule was heated up by an induction furnace. Eventually, YbCo₂ were obtained by reacting the Co powder with the melted Yb for 20-30 minutes. The cubic MgCu₂-type structure was confirmed by the X-ray powder diffraction. The ratio of Yb : Co in the sample were 1 : 2.03(1) determined by the electron-probe microanalysis.

Specific heat was measured down to 0.4 K by a ³He option of PPMS (Quantum Design Co.) by the thermal relaxation method. Measurements at lower temperatures down to 0.1 K were conducted by using a laboratory-made calorimeter installed in the commercial Cambridge Magnetic Refrigerator mFridge in the magnetic field up to 4 T. Magnetization was measured down to 1.8 K and up to 5 T by MPMS (Quantum Design Co.). We measured magnetization down to 0.4 K by a capacitive Faraday magnetometer installed in a ³He single-shot refrigerator (Heliox, Oxford Instruments)^{23,24}. The ADR experiments were performed by a laboratory-made ADR cell attachable to PPMS. The setup and the procedure of our ADR experiments are described in Ref. [19].

Figure 1(a) shows the electronic specific heat divided by temperature, C_{el}/T , as a function of temperature in the magnetic field up to 8 T. C_{el} is obtained as $C_{el} = C - C_{nuc} - C_{ph}$, where C , C_{nuc} , and C_{ph} are the raw data of the specific heat, nuclear, and phonon contributions, respectively. In Fig. S1 of

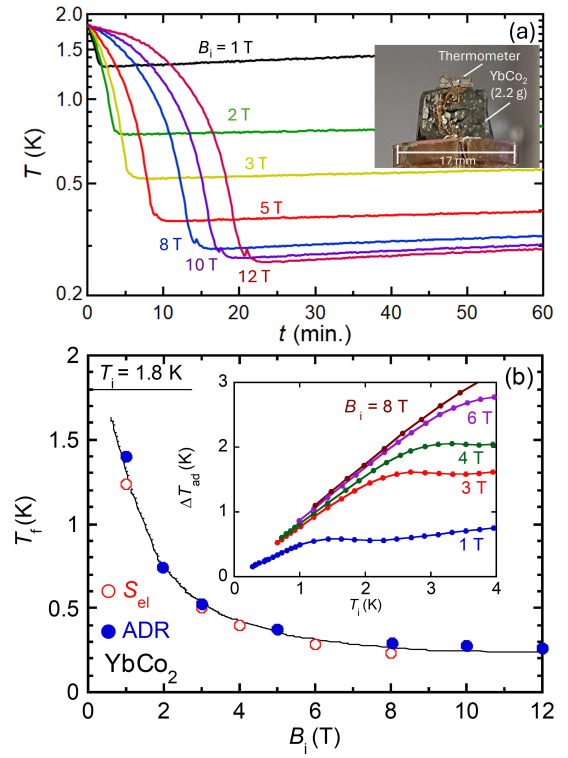


FIG. 2. (a) Time dependence of temperature in YbCo₂ by ADR from the initial temperature of $T_i = 1.8$ K and the various initial fields of $B_i = 1, 2, 3, 5, 8, 10,$ and 12 T. The inset shows the picture of the sample used in this ADR experiment. This sample was mounted on the laboratory-made ADR cell attachable to PPMS¹⁹. (b) Final temperature T_f from $T_i = 1.8$ K as a function of B_i . T_f are determined by the electronic entropy S_{el} in Fig. 1(b) (Open Circles) and the ADR experiment (Closed Circles). The inset displays the adiabatic temperature change $\Delta T_{ad} = T_i - T_f$ which is derived from S_{el} in Fig. 1(b).

the Supplementary Material, we plot C/T and C_{ph}/T where C_{ph} extract from Ref. [21] is the specific heat of the non-magnetic reference compound YNi₂. In this paper, we focus on the low-temperature range below 6 K where C_{ph} is ignorable small, compared with C_{el} . In the magnetic fields up to 4 T, we observed a convex downward curvature in C/T below ~ 0.3 K as shown in Fig. S1. This curvature following $C_{nuc}/T \sim 1/T^3$ is subtracted from C/T .

As shown by the solid arrows in Fig. 1(a), a drop in C_{el}/T on heating is observed above 1 T and 2 K. As observed and discussed in Ref. [21, 22], this drop is due to the field-induced phase transition whose phase boundary is plotted in the inset of Fig. 3(b). In addition, as indicated with the open arrows in Fig. 1(a), a sharp peak suggesting another phase transition is observed at 0.3 K at zero field. This peak is proposed to be the magnetic order because the internal field is observed below 0.4 K in the muon spin resonance experiments²². Figure 1(b) displays the temperature dependence of the electronic entropy S_{el} derived by integrating $C_{el}(T)/T$ with respect to the

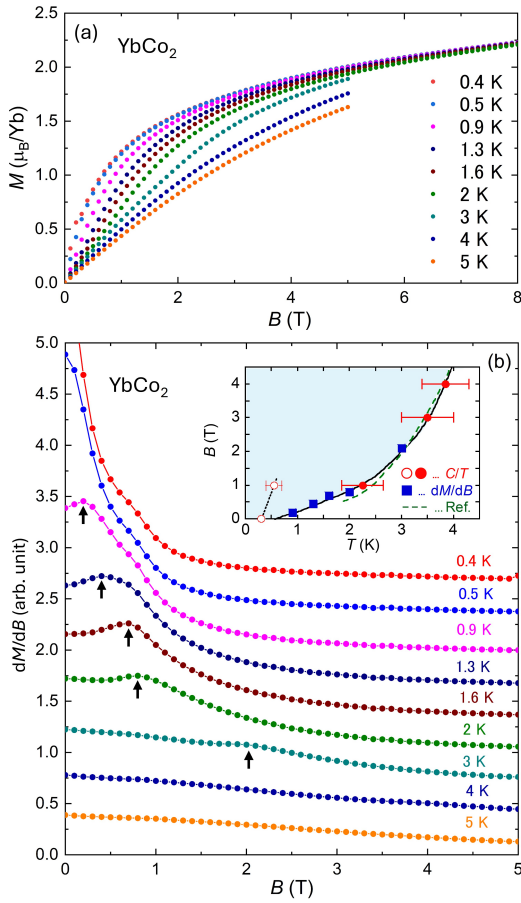


FIG. 3. (a) Magnetic field dependence of magnetization M down to 0.4 K up to 8 T in YbCo_2 . (b) Field derivative of magnetization dM/dB . The peaks by the metamagnetic transition are indicated by the arrows. The inset shows the magnetic phase diagram constructed from the peaks in dM/dB (squares), the peaks (open circles) and the drops (closed circles) observed in C_{el}/T in Fig. 1(a). The dashed green line shows the phase boundary reported in Ref. [21].

temperature. At zero field, $S_{el}(T)$ reaches $R \ln 2$ J/Kmol at ~ 1 K resultant from the Kramers doublet of a Yb^{3+} ion. As described later, $-\Delta S_M$ and ΔT_{ad} are obtained from S_{el} at zero field and the magnetic field.

Figure 2(a) displays the time dependence of the sample temperature in the ADR experiments from $T_i = 1.8$ K with various initial fields up to $B_i = 12$ T. Demagnetization from $t = 0$ was performed with a speed of 0.6 T/min. The YbCo_2 sample with 2.2 gram mass was mount on a Cu-stage which is thermally insulated from the heat bath at 1.8 K as shown in the inset of Fig. 2(a). The temperature of the sample measured by an attached RuO_2 thermometer exhibits a minimum after demagnetization. This minimum temperature is T_f from $T_i = 1.8$ K by ADR. In Fig. 2(b), we plot the B_i dependence of T_f obtained from our ADR experiments and those evaluated from S_{el} in Fig. 1(b). Here, T_f is defined as the temperature at the intersection between $S_{el}(T, B = 0)$ and a line parallel to the horizontal (temperature) axis from $S_{el}(T = T_i, B \neq 0)$.

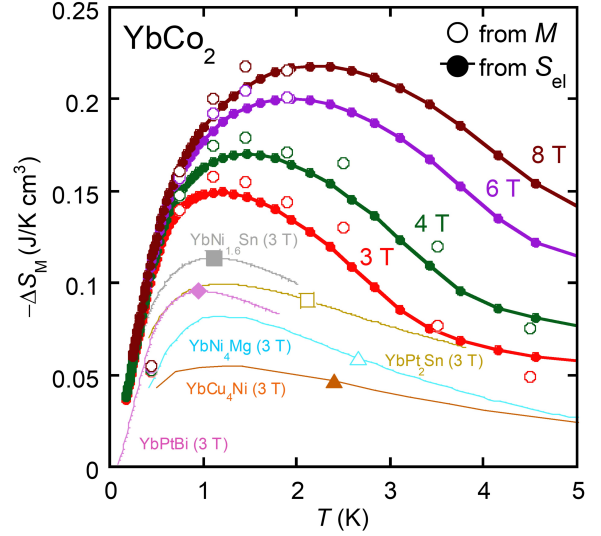


FIG. 4. The magnetic entropy change per volume $-\Delta S_M$ as a function of temperature, determined by the magnetization M in Fig. 3 and the electronic entropy S_{el} in Fig. 1. For comparison, we also plot $-\Delta S_M$ in the reported Yb-based metallic magnetic refrigerants for sub-Kelvin temperature under the magnetic field of 3 T^{13–16,25}. In YbPt_2Sn , the average of entropy at 2 T and 4 T is adopted as entropy at 3 T¹³.

These two T_f evaluated from S_{el} and the ADR experiments well overlap with each other. T_f decreases with increasing B_i and reaches 0.26 K at 12 T. The adiabatic temperature change $\Delta T_{ad} = T_i - T_f$ evaluated from S_{el} is displayed in the inset of Fig. 2(b) as a function of T_i .

Figure 3(a) and (b) display the magnetic-field dependence of the magnetization M and the field derivative dM/dB down to 0.4 K, respectively. The value of M even above 5 T is $\sim 2 \mu_B/\text{Yb}$ which is about half of $4.00 \mu_B/\text{Yb}$ expected from the Yb^{3+} free ion without the crystalline-electric-field effect. dM/dB in Fig. 3(b) exhibits a peak due to the metamagnetic transition between 0.9 K and 3 K as shown by the arrows. In the inset of Fig. 3(b), we show the $B - T$ phase diagram constructed with the peak in dM/dB , the drop due to the field-induced phase transition above 2 K, and the peak below 0.5 K in C_{el}/T of Fig. 1(a). This phase boundary of the field-induced phase transition is almost consistent with the reported one²². Notably, absence of the peak in dM/dB below 0.5 K suggests this phase boundary reaches the finite temperature in the zero magnetic field.

From two different measurements of specific heat and magnetization, $-\Delta S_M$ individually can be evaluated as shown in Fig. 4. Through the Maxwell relation of $(\partial S/\partial B)_T = (\partial M/\partial T)_B$, $-\Delta S_M$ as a function of B at a temperature $T = (T_1 + T_2)/2$ is derived from a pair of the isothermal magneti-

zation data at two temperatures of T_1 and T_2 as,

$$-\Delta S_M(B, T) = - \int_0^B \frac{dM(B', T)}{dT} dB' \\ \cong - \int_0^B \frac{M(B', T_1) - M(B', T_2)}{T_1 - T_2} dB'.$$

$-\Delta S_M(T)$ evaluated from the magnetization in Fig. 3(a) is plotted by the open circles in Fig. 4. $S_{el}(T)$ obtained from the specific heat data in Fig. 1 also provides $-\Delta S_M(B) = S_{el}(B = 0) - S_{el}(B)$ as a function of temperature. At 3 T, $-\Delta S_M(T)$ derived from the specific heat and magnetization data exhibits a peak around 1 K, where the value of $-\Delta S_M$ is ~ 0.15 J/K cm^3 . This peak goes to the higher temperature side with increasing magnetic fields. For comparison, we plot $-\Delta S_M(T)$ at 3 T in the reported Yb-based metallic magnetic refrigerants to provide sub-Kelvin temperature^{13–16,25}. The coexistence of the largest $-\Delta S_M(T)$ of YbCo₂ among them and T_f below 0.3 K as shown in Fig. 2 indicate the utilities as the cryogenic magnetic refrigerants. As the magnetic refrigerants exhibiting T_f below ~ 1 K and evidently exceeding $-\Delta S_M \sim 0.15$ J/K cm^3 around 3 T, some rare-earth oxides/fluorides of the insulators have been reported^{3,5,6,8}. Notably, $-\Delta S_M \sim 0.2$ J/K cm^3 has been reported in a Er($4f^{11}$)-based intermetallic compound ErPd₂Sb²⁶.

Materials containing high-density magnetic atoms like YbCo₂ are expected to possess a large $-\Delta S_M$ per volume. However, in general, since the strength of the magnetic interaction or magnitude of T_M is correlated with the density of magnetic ions, such a large $-\Delta S_M$ competes with the low $T_M \approx T_f$ below 1 K. The field-induced order in YbCo₂ is sufficiently suppressed by decreasing the magnetic field to zero, as shown in the inset of Fig. 3(b). In other words, YbCo₂ at zero field is located around the boundary between the magnetically ordered phase and the paramagnetic disordered one as the magnetic quantum critical point. This suppression of T_M results in the low T_f even in the high-Yb-density environment. Indeed, the minimization of T_f is observed in the vicinity of the boundary between magnetically ordered phase and paramagnetic disordered one by substituting Cu with Ni in an antiferromagnet Ce₂Cu₂In¹⁹. In addition, since emergence of field-induced order in YbCo₂ suppresses the entropy under the magnetic field $S_{el}(B \neq 0)$, this field-induced order contributes to increase of $-\Delta S_M = S_{el}(B = 0) - S_{el}(B \neq 0)$. Thus, the large $-\Delta S_M(T)$ can coexist with the low T_f below ~ 1 K because the ground state at zero field is located around the boundary between the field-induced ordered phase and paramagnetic one.

In conclusion, we report the performance of a Yb-based intermetallic compound YbCo₂ as the magnetic refrigerants for cooling down to sub-Kelvin temperature by measuring the specific heat and magnetization, in addition to the ADR experiments. The magnetic entropy change $-\Delta S_M(T)$ per volume exhibits a maximum in $B = 3$ T at ~ 1 K, where the value of $-\Delta S_M$ is ~ 0.15 J/K cm^3 . This value is particularly large in the reported Yb-based intermetallic magnetic refrigerants for sub-Kelvin temperature. The large $-\Delta S_M(T)$ and the low T_f below 0.3 K are attributed to the ground state, at zero field, locating around the boundary between the field-induced ordered

phase and paramagnetic one.

In Supplementary Material, we show the raw data of the specific heat before subtracting the nuclear and lattice contribution.

This work was financially supported by the JST FOREST Program (Grant Number JPMJFR2233) and JSPS KAKENHI (Grant Numbers JP22K03529, 23H04866, 23H04870, and 24K21692). YS thanks the Japanese research grants from "The Kyoto Technoscience Center" (No. 8 in 2024), and "The Mazda Foundation" (No. 21KK-191). The measurements at the cryogenic temperature and composition analysis were performed at N-BARD in Hiroshima University. We acknowledge for the useful comments by Yoshifumi Tokiwa and Toshiro Takabatake.

AUTHOR DECLARATIONS

CONFLICT OF INTEREST

The authors have no conflicts to disclose.

AUTHOR CONTRIBUTIONS

Yasuyuki Shimura: Conceptualization (lead); Investigation (supporting); Data curation (supporting); Writing - original draft (lead); Writing - review & editing (equal); Supervision (lead). **Ryoma Yokoo:** Investigation (lead); Data curation (lead); Writing - review & editing (equal). **Kanta Watanabe:** Investigation (supporting); Data curation (supporting); Writing - review & editing (equal). **Hiroto Furuie:** Investigation (supporting). **Naohito Tsujii:** Conceptualization (supporting); Writing - review & editing (equal). **Kazunori Umeo:** Investigation (supporting); Writing - review & editing (equal). **Takahiro Onimaru:** Investigation (supporting); Writing - review & editing (equal).

DATA AVAILABILITY

The data that support the findings of this study are available within the article and the supplementary material.

REFERENCES

- ¹O. E. Vilches and J. C. Wheatley, "Measurements of the specific heats of three magnetic salts at low temperatures," *Phys. Rev.* **148**, 509 (1966).
- ²F. Pobell, *Matter and Methods at Low Temperatures* (Springer-Verlag Berlin Heidelberg, 1992).
- ³B. Daudin, R. Lagnier, and B. Salce, "Thermodynamic properties of the gadolinium gallium garnet, Gd₃Ga₅O₁₂, between 0.05 and 25 K," *J. Magn. Mater.* **27**, 315–322 (1982).
- ⁴T. Numazawa, K. Kamiya, P. Shirron, M. DiPirro, and K. Matsumoto, "Magnetocaloric effect of polycrystal GdLiF₄ for adiabatic magnetic refrigeration," *AIP Conf. Proc.* **850**, 1579–1580 (2006).

- ⁵P. Liu, D. Yuan, C. Dong, G. Lin, E. G. Villora, J. Qi, X. Zhao, K. Shimamura, J. Ma, J. Wang, Z. Zhang, and B. Li, “Ultralow-field magnetocaloric materials for compact magnetic refrigeration,” *NPG Asia Mater.* **15**, 41 (2023).
- ⁶E. Palacios, J. A. Rodríguez-Velamazán, M. Evangelisti, G. J. McIntyre, G. Lorusso, D. Visser, L. J. de Jongh, and L. A. Boatner, “Magnetic structure and magnetocalorics of GdPO₄,” *Phys. Rev. B* **90**, 214423 (2014).
- ⁷A. Jesche, N. Winterhalter-Stocker, F. Hirschberger, A. Bellon, S. Bachus, Y. Tokiwa, A. A. Tsirlin, and P. Gegenwart, “Adiabatic demagnetization cooling well below the magnetic ordering temperature in the triangular antiferromagnet KBaGd(BO₂)₃,” *Phys. Rev. B* **107**, 104402 (2023).
- ⁸Z. W. Yang, J. Zhang, B. Liu, X. Zhang, D. Lu, H. Zhao, M. Pi, H. Cui, Y.-J. Zeng, Z. Pan, Y. Shen, S. Li, and Y. Long, “Exceptional magnetocaloric responses in a gadolinium silicate with strongly correlated spin disorder for sub-kelvin magnetic cooling,” *Adv. Sci.* **11**, 2306842 (2024).
- ⁹T. Treu, M. Klinger, N. Oefele, P. Telang, A. Jesche, and P. Gegenwart, “Utilizing frustration in Gd- and Yb-based oxides for milli-kelvin adiabatic demagnetization refrigeration,” *J. Phys.: Condens. Matter* **37**, 013001 (2024).
- ¹⁰Y. Tokiwa, S. Bachus, K. Kavita, A. Jesche, A. A. Tsirlin, and P. Gegenwart, “Frustrated magnet for adiabatic demagnetization cooling to milli-Kelvin temperatures,” *Commun. Mater.* **2**, 42 (2021).
- ¹¹U. Arjun, K. Ranjith, A. Jesche, F. Hirschberger, D. Sarma, and P. Gegenwart, “Efficient adiabatic demagnetization refrigeration to below 50 mK with ultrahigh-vacuum-compatible Ytterbium diphosphates AYbP₂O₇ (A = Na, K),” *Phys. Rev. Appl.* **20**, 014013 (2023).
- ¹²A. Liu, J. Zhou, L. Wang, Y. Cao, F. Song, Y. Han, J. Li, W. Tong, Z. Xia, Z. Ouyang, J. Zhao, H. Guo, and Z. Tian, “Large magnetocaloric effect in the shastry-sutherland lattice compound Yb₂Be₂GeO₇ with spin-disordered ground state,” *Phys. Rev. B* **110**, 144445 (2024).
- ¹³D. Jang, T. Gruner, A. Steppe, K. Mitsumoto, C. Geibel, and M. Brando, “Large magnetocaloric effect and adiabatic demagnetization refrigeration with YbPt₂Sn,” *Nat. Commun.* **6**, 8680 (2015).
- ¹⁴T. Gruner, J. Chen, D. Jang, J. Banda, C. Geibel, M. Brando, and F. M. Grosche, “Metallic local-moment magnetocalorics as a route to cryogenic refrigeration,” *Commun. Mater.* **5**, 63 (2024).
- ¹⁵X. Zhang, T. Zhang, Z. Zhuang, Z. Leng, Z. Wei, X. Liu, J. Xiang, S. Zhang, and P. Sun, “YbNi₄Mg: Superheavy fermion with enhanced wilson ratio and magnetocaloric effect,” *Phys. Rev. Mater.* **9**, 014402 (2025).
- ¹⁶Y. Shimura, K. Watanabe, T. Taniguchi, K. Osato, R. Yamamoto, Y. Kusanose, K. Umeo, M. Fujita, T. Onimaru, and T. Takabatake, “Magnetic refrigeration down to 0.2 K by heavy fermion metal YbCu₄Ni,” *J. Appl. Phys.* **131**, 013903 (2022).
- ¹⁷Y. Tokiwa, B. Piening, H. S. Jeevan, S. L. Bud’ko, P. C. Canfield, and P. Gegenwart, “Super-heavy electron material as metallic refrigerant for adiabatic demagnetization cooling,” *Sci. Adv.* **2**, e1600835 (2016).
- ¹⁸J. G. Sereni, “Thermomagnetic properties of very heavy fermions suitable for adiabatic demagnetisation refrigeration at low temperature,” *Philos. Mag.* **100**, 1211 (2020).
- ¹⁹K. Watanabe, Y. Shimura, K. Umeo, T. Onimaru, and T. Takabatake, “Minimization of temperature reached by adiabatic demagnetization refrigeration in Ce-based intermetallic Ce₂(Cu_{1-x}Ni_x)₂In,” *Appl. Phys. Lett.* **126**, 092401 (2025).
- ²⁰K. Buschow, “Note on the structure and occurrence of ytterbium transition metal compounds,” *J. Less Common Met.* **26**, 329–333 (1972).
- ²¹J. Valenta, N. Tsujii, H. Yamaoka, F. Honda, Y. Hirose, H. Sakurai, N. Terada, T. Naka, T. Nakane, T. Koizumi, H. Ishii, N. Hiraoka, and T. Mori, “Unusually strong electronic correlation and field-induced ordered phase in YbCo₂,” *J. Phys.: Condens. Matter* **35**, 285601 (2023).
- ²²J. Valenta, M. Klicpera, N. Tsujii, M. Hase, P. Proschek, J. Prokleka, J. R. Hester, Y. Matsuo, H. Sakurai, G. D. Morris, B. Hitti, R. Palm, M. Mansson, I. Umegaki, K. Ohishi, J. Sugiyama, T. Mori, and J. Katil, “Magnetic structure and phase diagram of YbCo₂; specific heat, muon spin rotation and relaxation and neutron diffraction study,” *J. Alloys Compd.* **1037**, 182352 (2025).
- ²³T. Sakakibara, H. Mitamura, T. Tayama, and H. Amitsuka, “Faraday force magnetometer for high-sensitivity magnetization measurements at very low temperatures and high fields,” *Jpn. J. Appl. Phys.* **33**, 5067 (1994).
- ²⁴Y. Shimizu, Y. Kono, T. Sugiyama, S. Kittaka, Y. Shimura, A. Miyake, D. Aoki, and T. Sakakibara, “Development of high-resolution capacitive faraday magnetometers for sub-kelvin region,” *Rev. Sci. Instrum.* **92**, 123908 (2021).
- ²⁵E. D. Mun, S. L. Bud’ko, C. Martin, H. Kim, M. A. Tanatar, J.-H. Park, T. Murphy, G. M. Schmiedeshoff, N. Dilley, R. Prozorov, and P. C. Canfield, “Magnetic-field-tuned quantum criticality of the heavy-fermion system YbPtBi,” *Phys. Rev. B* **87**, 075120 (2013).
- ²⁶Z. Chen, X. Liu, J. Shen, G. Zhang, H. Tu, J. Xiang, X. Zheng, X. Liu, X. Kan, W. Li, and D. Wang, “Large magnetocaloric effect in triangular antiferromagnet ErPd₂Sb,” *Appl. Phys. Lett.* **126**, 152408 (2025).